FREQUENCY DOMAIN SPECTRAL HAND VEIN PATTERNS AUTHENTICATION

A. M. Badawi[1], M. K. Shahin[2]
[1]Biomedical Engineering Department, University of Tennessee, Knoxville, TN, USA
[2]Suez Canal Authority Hospital - Ismaillia, Egypt
e-mail: ambadawi@utk.edu

oAbstract- **In this paper a hand vein pattern authentication based on the frequency domain patterns correlation is presented. Correlation matching based on the hand vein pattern frequency domain spectrum is analyzed. In order to evaluate the system testing performance, a dataset of 50 persons of different ages above 16 and of different gender, each has 10 images per person was acquired at different intervals, 5 images for left hand and 5 images for right hand. In verification testing analysis we used 3 images to represent the templates and 2 images to test. Each image is matched with the existing 3 templates. We found that our system can operate at 72.72 percent genuine acceptance rate and a 0.047 percent false acceptance rate, and the corresponding threshold is 91. The system's testing EER is 10.19 percent at threshold 87. For the 300*300 templates, the optimal threshold is 91 with FAR of 0.046 and FRR of 22.56. For the testing phase, matching the 200 test patterns with the 300 templates of 100 hands, the optimal threshold is 91 with FAR of 0.136 and FRR of 13.5 with EER of 3 percent at threshold 89. The system efficiency at this threshold was found to be 99.73%.**
***Keywords*- Biometrics, Verification, Hand Veins, FFT, Statistical Performance.**

I. INTRODUCTION

Authenticating the identity of an individual using vein patterns was investigated by several authors [1-5]. The infrared region is of special advantage since the skin tissue is relatively transparent and the blood absorbs infrared light well. Hence, the image contrast is higher than in the visible area. Since the arrival of fairly low cost CCD cameras and computer power, it seems straightforward to try to consider these technologies [6-7]. There are many research attempts for the extraction, segmentation and tracing of subcutaneous peripheral venous patterns [8-11], its main aim is to make data reduction and noise suppression for good diagnostic purposes and for making some quantitative measurements like lengths and diameters for the extracted vessel segments. These techniques based on mathematical morphology and curvature (veins direction) evaluation for the detection of vessel patterns in a noisy environment. Researchers in hand vein biometrics [1-5] had a satisfactory result for either verification or identification purposes, regardless of the difference in datasets size, methods, or vein similarities used. The vein tree detection stage includes four consecutive sub stages, which are hand region segmentation (i.e. region of interest localization and background elimination), smoothing and noise reduction, local thresholding for separating veins, and postprocessing. In literature of hand vein biometrics, Tanaka et al [3] have used phase only correlation to match two hand vein images, however he was working directly on the grayscale pattern of hand vein without extraction of that unique pattern. In this paper, we propose a method for correlation of hand vein patterns using frequency domain spectral matching.

II. DATA ACQUISITION AND PROCESSING

A monochrome frame-grabber is used to capture an image of the back of a hand for computer processing. Images are captured using a 320W X 240H pixels of 8-bits per pixel. A sample image is shown in Fig.1 for a male hand. A dataset of 50 persons of different ages above 16 and of different gender, each has 10 images per person was acquired at different intervals, 5 images for left hand and 5 images for right hand. The data set is for normal persons who do not complain from any diseases such as arthritis.

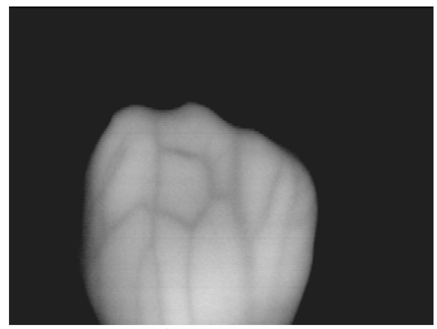

Fig.1. Acquired image of 320W X 240H pixels, 8-bits per pixel

A. Hand Vein Image Processing Stages

This is the second stage in the Hand Vein Verification System (HVVS), which covers the detection of vein structures from the acquired infrared image for the back of the hand. The vein tree detection stage includes four steps, which are hand region segmentation (i.e. region of interest localization and background elimination), smoothing and noise reduction, local thresholding for separating veins and finally the postprocessing.

B. Hand Region Segmentation

Image segmentation is one of the most important steps leading to the analysis of processed image data. Its main goal is to divide an image into parts that have a strong correlation with objects or areas of the real world contained in the image. Binarization is the case of segmenting the image into two levels; object (hand region) and background; the object segment which is the region of interest (ROI) in white and the background segment in black as shown in Fig. 2. The algorithm used in the segmentation sub stage is an iterative method used for calculating and selecting an optimal threshold, which is used to segment the image into two distinct parts; hand and background [13]. We used this resultant binary image to calculate the center of gravity (COG) for our ROI (hand region). Then we translated the

grayscale hand region to the center of the image after assigning the background area to zero value pixels. Thus we completely localized, separated and centered the hand region for subsequent processing steps.

Fig.2. Segmentation results; (a) Input gray scale image (b) Binary image and (c) Output image after ROI determination and centering

C. Smoothing and Noise Reduction

Two approaches could be used for noise filtering. First approach is using Gaussian smoothing filter. The disadvantage of Gaussian filter is its non-edge preserving ability, since it blurs the image with equal weights; also edges of the veins are blurred and completely diffuse after several smoothing iterations. The second approach is an edge-preserving technique like nonlinear diffusion [16-17]; in which the image gradient was used to weight the diffusion process. Fig. 3 show results of the smoothing filters used in this work where we used a median filter of 5*5 mask in order to remove the hand traces from the acquired image then we used the nonlinear diffusion filter based on edge weighted diffusion in order to smoothen the image while preserving the vein edges. The smoothing and noise cleaning sub stage effect is shown in Fig. 3 for 5 iterations of nonlinear diffusion, while the edges are not affected.

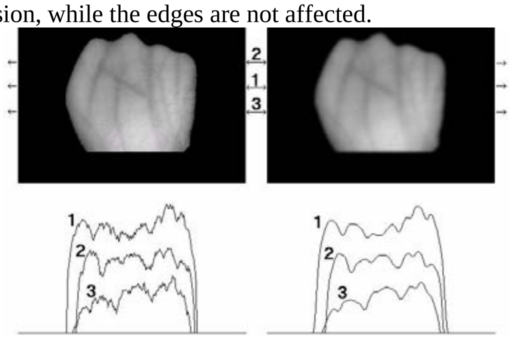

Fig.3. Effect of smoothing sub stage on the image line profiles

D. Hand Vein Pattern Segmentation

Specifically, hand vein segmentation is to divide a hand vein image into a foreground (veins in the back of the hand) and a background (non-vessel areas). Segmentation methods can be divided into four groups, which are threshold-based segmentation, edge based segmentation, region based segmentation and segmentation by matching. In this study, the first thresholding method is adopted since it is computationally cheap and fast. Considering that we want to process and study veins only, global thresholding (i.e. single threshold for the whole image) is not a good technique for this purpose. A better approach is to calculate the average around each pixel of the image in an area of NxN neighbor pixels and to use average value as a threshold value [11]. The local threshold process separates the vein pattern from the background; hence the desired vein image is extracted. Experimentally we have chosen a 31x31 mask size for computing the threshold for binarizing the central pixel. The result is shown in Fig. 4.

Fig.4. Processed image (left) and its local thresholded image (right)

E. Hand Vein Pattern Postprocessing

It is demonstrated from Fig. 4 that the resultant binary hand vein contains some noise and un-sharp edges. We experimentally applied 5x5 median filter for improving and validating the output binary hand vein pattern and for reducing the effect of these unwanted defects [13]. We also converted the vein pattern into white in a black background which in this case the entire image. The final pattern after the post processing sub stage is shown in Fig. 5.

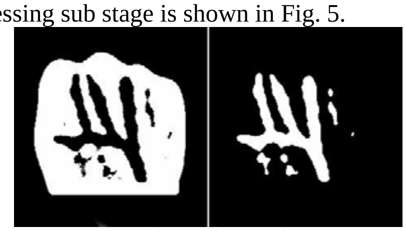

Fig.5. Hand vein pattern before (left) and after postprocessing (right)

F. Frequency Domain Analysis of Hand Vein Patterns

The resulted image after preprocessing was transformed using FFT. Example of FFT spectral image for a grayscale pattern is shown in Fig. 6. Most of spectral patterns are star like shapes. Star rays differ in size, shapes, and orientation about central axes. Information extracted from frequency domain from the star patterns can be later used in hand veins frequency domain patterns type classification.

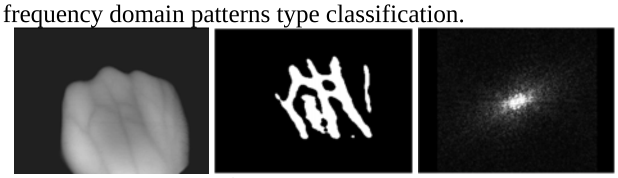

Fig.6. Grayscale vein (left), Pattern (Middle) and FFT spectrum (right)

G. Matching of Hand Vein Patterns in Frequency Domain

After image acquisition and hand vein extraction sub stages, we have a binary image contains the segmented vein pattern of the back of the hand. The Fourier transform for this binary image was calculated using the Fast Fourier transform (FFT) algorithm; the 2-D Discrete Fourier Transform (DFT) is demonstrated in equation (1). We calculated the Fourier Spectrum for the resulted patterns using equation (2) [13].

$$F(u,v) = \sum_{x=0}^{M-1}\sum_{y=0}^{N-1} f(x,y)e^{-j2\pi(ux/M+vy/N)} \tag{1}$$

$$|F(u,v)| = [R^2(u,v) + I^2(u,v)]^{1/2} \tag{2}$$

This is suitable for the next and the final sub stage, the matching of hand vein patterns in frequency domain. As it is expected, the input for the matching sub stage is two hand vein spectral images like the one in Fig. 6 (right), the matching output is Yes (the two images are for the same pattern) or No (the input images is not correlated). We performed a normalized cross correlation between the two spectral images to get a normalized spectral similarity ratio between the two spectral patterns. Since frequency domain spectrum is invariant to translations in spatial domain. We address only rotation in registration technique to find the maximum spectral correlation [14]. We have already constrained our data acquisition system with the hand attachment in order to prevent any rotation. One of the two spectral images is remained stationary while we apply 2D transformation (rotation) on the other image in order to align it with the first pattern (Registration) to find the maximum correlation percentage between two hand vein spectral images [22-24].

$$Correlation(\theta) = \underset{\theta}{Forall}(|X| * |T| * 100) / Min(|X|^2, |T|^2) \quad (3)$$

$$MaxCorrelation = Max(Correlation(\theta)) \quad (4)$$

Where |X| is an image contains FT spectrum of the first test hand vein pattern, |T| is the second image contains FT spectrum of the transformed template hand vein pattern, * is the ordinary multiplication mathematical operator, Min ($|X|^2$,$|T|^2$) is the minimum value of the summation of the spectrum square between the two patterns to be matched.

However Fujitsu researchers have presented a contactless/touchless palm vein authentication which is more convenient and non hygienic for users we restricted our designed prototype for a contact system type in order to simplify our matching phase and derive a dependent statistical measures for this proposed prototype. However accounting for scale (Age or hand to camera distance) in the registration algorithm is simple to implement in frequency domain, we did not account for the scale in our matching method. In real systems capturing the hand template at equal monthly intervals after correct authentication is suggested in order to track the changes in the hand with age. The matching (similarity) percentage is calculated cross correlation between the two images spectrum. We calculated the matching ratio for each transformation step then we choose the maximum ratio as the final matching ratio between the two input hand vein spectral patterns. In our implementation and for saving time of matching, we made the rotation parameter (rotation) steps equals five degree in frequency domain, getting the maximum matching ratio on this grid, finally we made a fine search (tune) to find the overall maximum correlation ratio. The result of matching sub-stage is shown in Fig. 7, in case of correct true match it is demonstrated that the resultant pattern is correlated to the input images and it is shown that the matching ratio is 94.00 % (same person). A case of correct mismatch is shown in Fig. 8, it is shown that the matching ratio is small as 73.43 % (different persons).

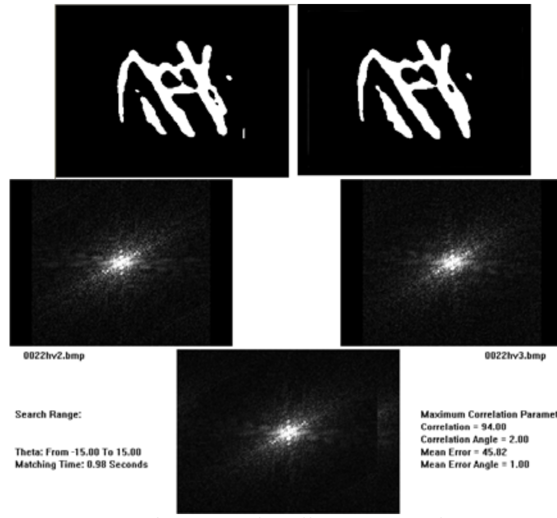

Fig.7. Example of true match for different patterns of the same person

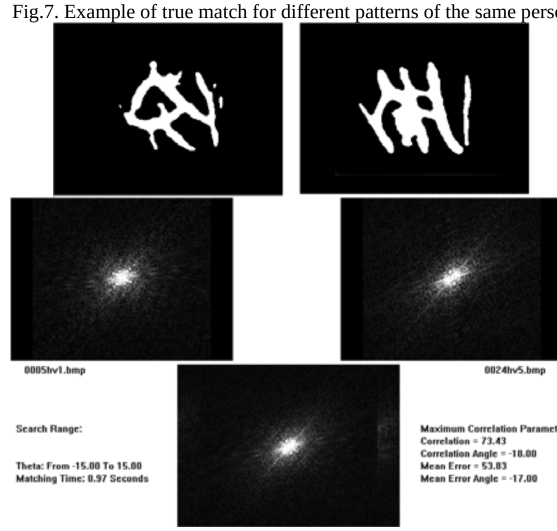

Fig.8. Example of correct mismatch between different persons

III. RESULTS

A. Statistical Results

The system was tested over a database collected using the designed system consisting of 50 persons of different age and gender for each 5 left and 5 right images were acquired. The person was asked to put his/her right hand on the hand attachment frame and the system operator captures the first image for the current person right hand veins. Then the person replaces his/her right hand with the left one for acquiring the first image for the left hand vein pattern. This process was repeated until we acquire five images for the right hand and five images for the left hand in different scenes (5 minutes interval between every acquired image) independent of each other, i.e. ten images for each person. We will prove in our statistical analysis that the hand vein pattern is unique to some level for each person and for each hand. Thus we considered as if we have 100 persons of which 5 images are in the dataset since we found that left and right hand vein images are different. In order to find the dissimilarity threshold in correlation ratio between the 100 subjects we have chosen only the first image pattern for each of the 100 subjects and for a correlation ratio threshold that

exceed 91%, we achieved 100% classification (Distinct pattern). For evaluating (testing) our system for verification purpose, all possible comparisons are made between the whole data. We matched each image from our data set with all the 500 hand vein images in our data set and then we recorded the matching ratios. We constructed the correlation matrix for representing the matching result between each image and all other images. We used the thresholded correlation matrix for calculating the efficiency of our system at each threshold. Also, we deduced that the optimal threshold at which the maximum efficiency occurs in our system. We performed statistical analysis for selecting an optimal threshold to get the highest system performance, by testing the system over the whole database - exhausting the whole database. To evaluate the hand vein performance we used measures of performance, which include: false accept rate (FAR), false reject rate (FRR), and efficiency. Fig. 11 shows how FAR(%), and FRR (%) change with different thresholds. Our aim is to select an optimal threshold. We want a single criterion, such that it takes into account the maximization of true events (GAR, GRR) and minimization of error events (FAR, FRR).

B. Verification Testing Results

To obtain the verification accuracy of our system, each of the images was matched with all of the images in the database after reducing it to 300 patterns (3 images for each hand instead of 5). A matching is noted as a correct matching if two images are from the same hand. The total number of matchings is 20000. The probability distributions for genuine and imposter are estimated by the correct and incorrect matchings, respectively, and are shown in Fig. 9. Fig. 10 depicts the corresponding Receiver Operating Characteristic (ROC) curve, for all possible operating points. From Fig. 10, we can see that our system can operate at a 86.5 percent genuine acceptance rate and a 0.136 percent false acceptance rate, and the corresponding threshold is 91. The system's testing equal error rate is 3 percent at threshold 89. In this verification testing analysis we used 3 images to represent the templates and 2 images to test. Each image is matched with the existing 3 templates. The same analysis for the 300*300 as in section A was repeated. Fig. 9-11 shows the results. For the 300*300 templates, the optimal threshold is 91 with FAR of 0.046 and FRR of 22.55. For the testing phase, matching the 200 test with the 300 templates of 100 hands, the optimal threshold is 91 with FAR of 0.136 and FRR of 13.5. The system efficiency at this threshold was found to be 99.73%. Fig. 11 shows FAR and FRR versus threshold.

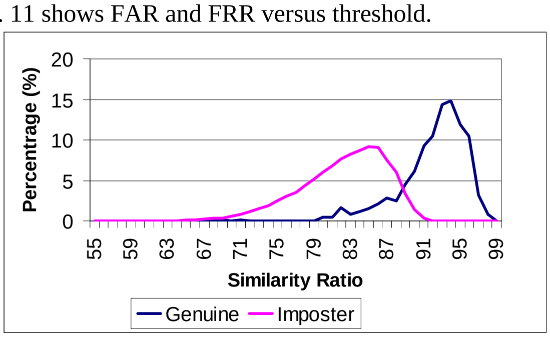

Fig 9. Verification test results for genuine and imposter distributions

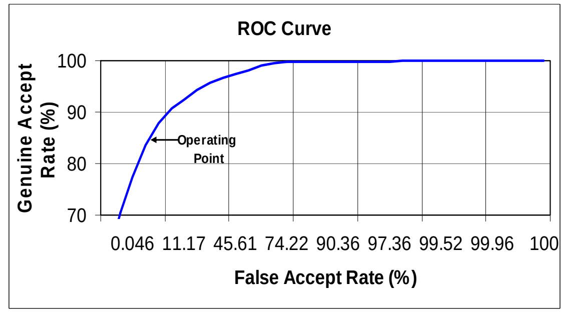

Fig 10. Verification test results the receiver operator characteristic curve.

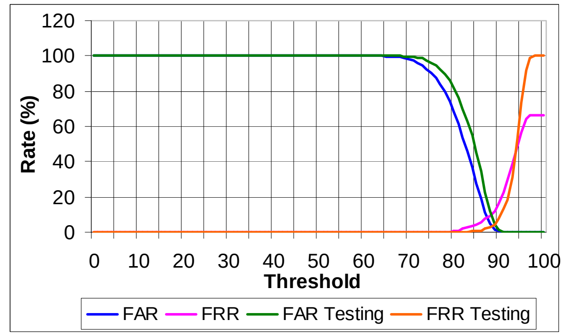

Fig 11. FAR & FRR for template and test analysis

IV. Discussion And Conclusion

The designed system was tested for verification purpose only over a database collected with the designed system. Dataset for 50 persons of different age and gender of which ten images per person were acquired (five for the right hand and five for the left) in different scenes at different intervals and are independent of each other, i.e. ten images for each person. Verification performance statistical parameters were estimated for the overall system such as: Genuine Accept Rate (Sensitivity), Genuine Reject Rate (Specificity), False Accept Rate (FAR), False Reject Rate (FRR), Efficiency and Receiver Operating Curve (ROC). System testing performance (overall efficiency) was found to be 99.73% at threshold (matching ratio) equal 91. At this maximum efficiency FAR of 0.136 and FRR of 13.5 were reported. However the difference in methods, datasets, and algorithms that were found in the hand biometric work of [1-5, 21], our performance results are comparable.

Acknowledgment

Dr. Mohamed S. Kamel at Systems and Biomedical Engineering, Cairo University and Dr. Mohamed R. Mahfouz at Biomedical Engineering Department, University of Tennessee, Knoxville are acknowledged for their assistance in prototype preparation, data acquisition phase, and valuable comments during the process of this study.

References

[1] J. M. Cross and C. L. Smith, "Thermographic Imaging of the Subcutaneous Vascular Network of the Back of the Hand for Biometric Identification", Proceedings of 29th

International Carnahan Conference on Security Technology, Institute of Electrical and Electronics Engineers, 20–35, 1995.
[2] S. Im, H. Park, Y. Kim, S. Han, S. Kim, C. Kang, and C. Chung, “A Biometric Identification System by Extracting Hand Vein Patterns”, Journal of the Korean Physical Society, 38(3): 268-272, March 2001.
[3] T. Tanaka and N. Kubo, “Biometric Authentication by Hand Vein Patterns” SICE, Annual Conference in Sapporo, 249-253, Aug. 2004.
[4] N. Miura, A. Nagasaka, and T. Miyatake, “Feature Extraction of Finger-Vein Patterns Based on Repeated Line Tracking and its Application to Personal Identification”, Machine Vision and Applications, 15: 194-203, 2004.
[5] C. Lin and K. Fan, “Biometric Verification Using Thermal Images of Palm-Dorsa Vein Patterns”, IEEE Transactions on Circuits and systems for Video Technology Vol. 14, No. 2, February 2004.
[6] O. Such, “Near Infrared Imaging of Hemodynamics”, Proceedings of 18th International Conference of the IEEE/EMBS, Amsterdam, Nov. 1996.
[7] O. Such, Sabine Acker, and Valdimir Blazek, “Mapped Hemodynamic Data Acquisition by Near Infrared CCD Imaging”, Proceedings of 19th International Conference of the IEEE/EMBS, Chicago, Oct. 1997.
[8] E. K. Y. Chan and J. A. Pearce, “A Rule-Based, Adaptive Window-Size Filter for the Enhancement of Subcutaneous Vascular Patterns in Thermographic Images”, Proceedings of 11th International Conference of the IEEE/EMBS, 1746-1748, Oct. 1989.
[9] K. Eric, Y. Chan and J. Pearce, “Visualization of Dynamic Subcutaneous Vasomotor Response by Computer-Assisted Thermography”, IEEE Transactions on Biomedical Engineering, 37(8): 786-795, August 1990.
[10] K. Eric, Y. Chan and J. Pearce, “A Computer-Assisted Thermography System for the Extraction, Visualization and Tracing of Subcutaneous Peripheral Venous Patterns”, IEEE International Symposium on Circuits and Systems, 1: 508 – 511, 1991.
[11] Y. Sun, “Automatic Identification of Vessel Contours in Coronary Arteries in Arteriograms by an Adaptive Tracing Algorithm”, IEEE Transactions on Medical Imaging, 8(1): 78-88, March 1989.
[12] F. Van Der Heijden, “Image Based Measurement Systems”, John Wiley & Sons, 1995.
[13] M. Sonka, V. Hlavac, and R. Boyle “Image Processing, Analysis and Machine Vision”, Chapman & Hall, 1993.
[14] R. Schalkoff, “Pattern Recognition: Statistical, Structural and Neural Approaches”, John Wiley & Sons, 1992.
[15] A. Papolis, “Probability, Random Variables and Stochastic Processes”, Third Edition, McGraw-Hill, New York, 1991.
[16] K. Abd-Elmoniem, A. Youssef, and Y. Kadah, “Real-Time Speckle Reduction and Coherence Enhancement in Ultrasound Imaging via Nonlinear Anisotropic Diffusion”, IEEE Transactions on Biomedical Engineering, 49(9): 997-1014, 2002.
[17] M. Rushdi, “Speckle Reduction in Medical Ultrasound Images Using Weighted Diffusion, Neural Networks, and Fuzzy Logic”, Master Thesis, Cairo University, Faculty of Engineering, 2005.
[18] S. Pankanti, S. Prabhakar, and A. Jain, “On the Individuality of Fingerprints”, IEEE Transactions on Pattern Analysis and Machine Intelligence, 24(8): 1010-1025, Aug. 2002.
[19] A. Jain, S. Prabhakar, L. Hong, and S. Pankanti, “Filterbank-Based Fingerprint Matching”, IEEE Transactions on Image Processing, 9(5): 846-859, 2000.
[20] A. Jain, L. Hong, and R. Bolle, “On-Line Fingerprint Verification”, IEEE Transactions on Pattern Anakysis and Machine Intelligence, 19(4): 302-314, 1997.
[21] R. Sanchez-Reillo, C. Sanchez-Avilla, and A. Gonzalez-Macros, “Biometrics Identification Through Hand Geometry Measurements”, IEEE Transactions on Pattern Anakysis and Machine Intelligence, 22(18): 1168-1171, 2000.
[22] http://homepages.inf.ed.ac.uk/rbf/HIPR2/hipr_top.htm
[23] S. Kruger, and A. Calway. “Image Registration using Multiresolution Frequency Domain Correlation”, British Machine Vision Conference, 2000.
[24] B.V. K. V. Kumar, M. Savvides, K. Venkataramani, and C. Xie, “Spatial Frequency Domain Image Processing for Biometric Recognition”, IEEE ICIP 2002.